

# Proposal for an experiment to verify Wigner's rotation at non-relativistic speeds with massive spin-1/2 particles

Veiko Palge\*

*Laboratory of Theoretical Physics, Institute of Physics,  
University of Tartu, W. Ostwaldi 1, 50411 Tartu, Estonia*

Jacob Dunningham†

*Department of Physics and Astronomy, University of Sussex, Brighton BN1 9QH, United Kingdom*

Yuji Hasegawa‡

*Atominstutut, Vienna University of Technology, Stadionalle 2, 1020 Vienna, Austria*

Christian Pfeifer§

*Center of Applied Space Technology and Microgravity (ZARM),  
University of Bremen, Am Fallturm 2, 28359 Bremen, Germany*

The Wigner rotation of quantum particles with spin is one of the fascinating consequences of interplay between special relativity and quantum mechanics. In this paper we show that a direct experimental verification of Wigner's rotation is in principle accessible in the regime of *non-relativistic* velocities at  $\sim 10^3 \text{ ms}^{-1}$  for massive spin-1/2 particles. We discuss how the experiment could be carried out in a laboratory using cold neutrons. The measurement at non-relativistic velocities becomes possible through letting neutrons propagate for a sufficiently long time because Wigner rotation is a cumulative effect.

## I. INTRODUCTION

Over the years, low-energy neutrons have proven to be invaluable in a range of experiments that probe foundational issues in physics [1–6]. They are useful test particles in interferometric, spectroscopic and scattering experiments probing low-energy scales and are a complementary tool to particle colliders. Their significance lies in providing direct tests of fundamental concepts to a high degree of accuracy. One area they might be usefully deployed is in precision measurements of the Wigner rotation, which first came to the fore in the context of atomic physics when Thomas showed that the hydrogen atom needs a relativistic correction due to a phenomenon that came to be called the Thomas precession [7]. In a nutshell, the Wigner rotation is a phenomenon that if a physical system undergoes non-collinear Lorentz boosts, then it is rotated relative to the original frame. Wigner's rotation also holds in the quantum domain and is experimentally confirmed in a plethora of phenomena from atomic spectra to particle acceleration. In the context of quantum information, it is the reason why the behavior of entanglement in relativity differs significantly from the standard, non-relativistic theory [8–12].

In this paper we propose an experiment to verify Wigner's rotation in the regime of what are typically regarded as non-relativistic velocities at  $\sim 10^3 \text{ ms}^{-1}$  in an implementation

with cold neutrons. This is significant because it would provide *direct* evidence of Wigner's rotation in the quantum domain in a system that can be carefully controlled and, because the experiment does not require relativistic speeds, it can be carried out in a laboratory. From a geometric point of view the experiment can be regarded as explicitly verifying the curvature of the relativistic velocity space—a feature that sets apart the relativistic and non-relativistic theories of spacetime [13].

The article is organized as follows. We begin by summarizing the theoretical derivation of the Wigner rotation in Sec. II followed by the discussion of the experimental setup with cold neutrons in Sec. III and the conclusion in Sec. IV.

## II. WIGNER ROTATION

Wigner's rotation originates in the fact that the subset of pure Lorentz boosts does not form a subgroup of the Lorentz group [14–16]. The combination of two boosts  $\Lambda(v_1)$  and  $\Lambda(v_2)$  is in general a boost *and* a rotation,

$$\Lambda(v_2)\Lambda(v_1) = W[\alpha(v_1, v_2)]\Lambda(v_3), \quad (1)$$

where, for massive spin-1/2 particles that we will focus on,  $W(\alpha) \in \text{SO}(3)$  is the Wigner rotation with angle  $\alpha$  about the axis  $\hat{n} = \hat{v}_2 \times \hat{v}_1$  orthogonal to the plane specified by  $v_1$  and  $v_2$ . This effect is a truly relativistic phenomenon both in the conceptual and quantitative senses. The latter means that in a simple scenario consisting of two boosts the rotation angle becomes significant at large velocities. For instance, if  $v_{1,2} = 0.5c$  and the velocities are orthogonal, then the rotation is 8 deg, while for non-relativistic speeds  $v_{1,2} = 2 \cdot 10^3 \text{ ms}^{-1}$  it is barely measurable at  $\sim 10^{-5}$  deg. However, one can achieve a measurable effect at low, non-relativistic velocities by noting another property of the Wigner rotation, namely,

\* Email: [veiko.palge@ut.ee](mailto:veiko.palge@ut.ee)

† Email: [J.Dunningham@sussex.ac.uk](mailto:J.Dunningham@sussex.ac.uk)

‡ Email: [hasegawa@ati.ac.at](mailto:hasegawa@ati.ac.at)

§ Email: [christian.pfeifer@zarm.uni-bremen.de](mailto:christian.pfeifer@zarm.uni-bremen.de)

that it is *cumulative*. This is because Wigner's rotation is ultimately a *holonomy*—a geometric phase that accumulates when a particle follows a path in the momentum space, in analogy to how Berry's phase accumulates when a particle follows a path in the parameter space associated with the Hamiltonian [13, 17, 18].

In the following, we will take the geometric approach [13], which is based on the fiber bundle theory [19, 20], and give an outline of how the Wigner angle can be calculated based on the idea that it is a geometric phase. We will then use the result to design an experiment that allows to measure the Wigner rotation of a particle at non-relativistic speeds.

From the intuitive point of view, in the fiber bundle picture we can think of the state of the massive relativistic spin-1/2 particle as a field on *curved* momentum space. When a particle is Lorentz boosted it follows a geodesic in this manifold. This means the spin of the particle is parallel transported along the geodesic. Because the momentum space is curved, the state of the particle in general changes non-trivially when it is parallel transported along a given path. Hence, the final state after completing parallel transport along a given path is generally not identical to the initial state. For closed paths, the transformation that maps the initial state to the final state is called a holonomy. The Wigner rotation is thus nothing but the holonomy which arises due to the curvature of the relativistic momentum space. We will next describe how to compute the holonomy transformation for a massive relativistic spin-1/2 particle.

In the fiber bundle theory, the quantum relativistic massive spin-1/2 particle is described by the spinor bundle  $(\pi : E \rightarrow \mathcal{V}_m^+, \mathcal{H}_p)$  where, using the sign convention  $\eta \sim$

$(+, -, -, -)$ ,  $\mathcal{V}_m^+$  is the forward mass hyperboloid  $\mathcal{V}_{m,x}^+ = \{P \in T_x^* \mathbb{E}^{1,3} \mid \eta(P, P) = \eta^{\mu\nu} p_\mu p_\nu = m^2, p_0 > 0\} \subset T_x^* \mathbb{E}^{1,3}$  and the typical fiber  $\mathcal{H}_p = \mathbb{C}^2$ , for a more detailed account see [13]. Because the Minkowski space is flat, we can identify the mass hyperboloids at different points of spacetime and speak of a single momentum hyperboloid  $\mathcal{V}_m^+$  in which the particle moves. Using the spherical polar coordinates, the intrinsic geometry of the momentum hyperboloid is described by the metric

$$g = - \left( \frac{m^2}{E^2} d\rho \otimes d\rho + \rho^2 d\theta \otimes d\theta + \rho^2 \sin^2 \theta d\phi \otimes d\phi \right). \quad (2)$$

In order to describe parallel transport, we compute the coefficients  $\omega^A{}_B$  of the spin connection using the relation

$$\omega^A{}_{Bi} = e^A{}_k e_B{}^j \Gamma^k{}_{ij} + e^A{}_k \partial_i e_B{}^k, \quad (3)$$

where  $e^A{}_i$  are components of an orthonormal coframe  $\Theta^A = e^A{}_i dz^i$  of the momentum space metric  $g$ . We can display  $\omega$  as the matrix

$$\omega = \begin{bmatrix} 0 & -\frac{E}{m} d\theta & -\sin \theta \frac{E}{m} d\phi \\ \frac{E}{m} d\theta & 0 & -\cos \theta d\phi \\ \sin \theta \frac{E}{m} d\phi & \cos \theta d\phi & 0 \end{bmatrix}. \quad (4)$$

We can likewise express the curvature of the Levi-Civita connection as a collection of 2-forms  $\Omega^A{}_B$  over  $\mathcal{V}_m^+$  written as the matrix

$$\Omega = \begin{bmatrix} 0 & -\frac{\sqrt{E^2 - m^2}}{Em} d\rho \wedge d\theta & -\frac{\sqrt{E^2 - m^2}}{Em} \sin \theta d\rho \wedge d\phi \\ \frac{\sqrt{E^2 - m^2}}{Em} d\rho \wedge d\theta & 0 & -\frac{(E^2 - m^2)}{m^2} \sin \theta d\theta \wedge d\phi \\ \frac{\sqrt{E^2 - m^2}}{Em} \sin \theta d\rho \wedge d\phi & \frac{(E^2 - m^2)}{m^2} \sin \theta d\theta \wedge d\phi & 0 \end{bmatrix}. \quad (5)$$

The state space of the particle is given as the space of square integrable sections  $\psi : \mathcal{V}_m^+ \rightarrow \mathbb{C}^2$  of the spinor bundle with a suitable representation of the group  $SU(2)$ . Formally, the spinor bundle is the associated bundle to the principal spin bundle whose structure group  $\text{Spin}(3) \cong SU(2)$  is the double cover of  $\text{SO}(3)$ .

In order to describe parallel transport of spinors, we need the spinor connection. This is induced by the Levi-Civita connection via lifting the  $\text{SO}(3)$  connection to the spin connection, and then generating the spinor connection. We get

$$\omega_s = -\frac{i}{2} \left( \frac{E}{m} d\theta \sigma^3 - \frac{E}{m} \sin \theta d\phi \sigma^2 + \cos \theta d\phi \sigma^1 \right). \quad (6)$$

Using the spinor connection, we calculate the spinor curvature

$$\Omega_s = d\omega_s + \omega_s \wedge \omega_s, \quad (7)$$

which yields

$$\begin{aligned} \Omega_s = & \frac{i}{2} \left( -\frac{\sqrt{E^2 - m^2}}{Em} d\rho \wedge d\theta \sigma_3 \right. \\ & + \frac{\sqrt{E^2 - m^2}}{Em} \sin \theta d\rho \wedge d\phi \sigma_2 \\ & \left. - \frac{E^2 - m^2}{m^2} \sin \theta d\theta \wedge d\phi \sigma_1 \right). \end{aligned} \quad (8)$$

Consider now a particle that follows circular path  $C$  in the momentum space. This means the particle is moving with constant speed  $v$ , but constantly changing its direction. One can think of particle's movement as undergoing infinitesimal parallel transports when it travels around the circular trajectory. Each small parallel transport corresponds to a small boost which gives rise to Wigner's rotation, all of which accumulate when the particle has completed one orbital revolution.

This corresponds to the famous case of Thomas precession, which is formally a holonomy associated with a circular path in the momentum space. The holonomy matrix can be calculated in terms of the spinor curvature  $\Omega_s$

$$\text{Hol}(\omega_s, C) = \exp \left( - \int_D \Omega_s \right), \quad (9)$$

where  $D$  is a disk with boundary  $C$  and the matrix is a function of connection  $\omega_s$  and path  $C$ . In our case, the path is a circle with radius  $\rho_0 \in \mathcal{V}_m^+$ , where  $\rho_0 = mv/\sqrt{1-v^2}$ . It is the boundary of the disc  $D$  given by  $\theta = \pi/2$ ,  $\rho \in (0, \rho_0)$  and  $\phi \in (0, 2\pi)$ . Using (8) with  $d\theta = 0$ , the integral

$$-\int_D \Omega_s = - \int_0^{\rho_0} \int_0^{2\pi} d\rho d\phi \frac{i}{2} \frac{\rho}{\sqrt{m^2 + \rho^2 m}} \sigma_2 \quad (10)$$

$$= -i\sigma_2\pi(\gamma(v) - 1). \quad (11)$$

By substituting into (9) we obtain the matrix

$$\text{Hol}(\alpha) = \exp \left( -i\frac{\alpha}{2}\sigma_2 \right) = \begin{pmatrix} \cos(\alpha/2) & -\sin(\alpha/2) \\ \sin(\alpha/2) & \cos(\alpha/2) \end{pmatrix}, \quad (12)$$

where we use the argument  $\alpha$  to emphasize that this is an  $\text{SU}(2)$  rotation matrix with an angle

$$\alpha(v) = 2\pi(\gamma(v) - 1) \quad (13)$$

which represents the holonomy transformation of the spin state after the particle has completed one revolution around  $C$ .

We will next describe an experiment that allows to measure Wigner's rotation using cold neutrons.

### III. EXPERIMENT

Consider a setup shown in Fig. 1 where a spin-1/2 particle with mass  $m$  and momentum  $|p\rangle$  comes in from the left with the initial spin prepared in state  $|\uparrow\rangle$ . We assume that the momentum and spin lie in the plane of the figure. The parti-

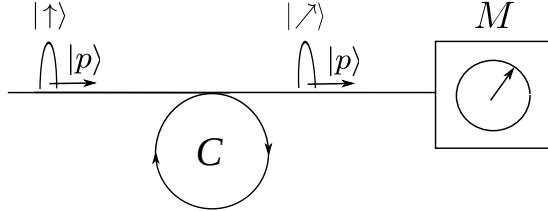


FIG. 1. Experimental setup for measuring Wigner rotation. Path of the particle is shown as solid line. The particle with momentum  $|p\rangle$  and spin  $|\uparrow\rangle$  enters from the left and follows circular path  $C$ . After each orbital revolution the spin is transformed by  $\text{Hol}(\alpha)$  resulting in rotation by angle  $\alpha$ . Letting the particle orbit  $N$  times produces the spin rotation by angle  $N\alpha$ . After this the particle in the rotated spin state  $|\nearrow\rangle$  exits towards the measurement apparatus  $M$  which measures the direction of spin.

cle then follows a path around circle  $C$  where it undergoes a series of small non-collinear boosts, each of which produces

a tiny Wigner rotation. The total Wigner angle accumulated as a result of a single orbital revolution around the circle at constant speed  $v$  is given by (13). While this angle is still too small for detection in practice, the effect can be amplified by letting the particle travel around the circle  $N$  times. This means the initial  $|\uparrow\rangle$  and final spin state  $|\nearrow\rangle$  of the particle are related by applying the holonomy transformation  $N$  times

$$|\nearrow\rangle = \text{Hol}(\alpha)^N |\uparrow\rangle = \text{Hol}(N\alpha) |\uparrow\rangle, \quad (14)$$

thus producing the total rotation angle  $N\alpha$ .<sup>1</sup>

A measurement  $M$  carried out on the final spin state shows the difference between the directions of the initial and final spins. Note that since we assumed that the initial spin lies in the plane of the circle or, equivalently, in the plane of the boosts around the circle, the particle undergoes maximal Wigner rotation.

#### A. Cold neutrons

Cold neutrons provide an interesting platform for realizing this experiment. They have been used extensively to probe fundamental concepts of quantum physics [6, 21–23]. The wavelength of cold neutrons ( $\sim 10^{-9} - 10^{-8}$  m) is larger than the distance between atoms and they mainly interact with the optical or Fermi pseudo potential  $V_F$  of matter [6]. We will therefore first analyze the magnitude of the effect using a model where neutrons are described in terms of neutron optics. Later in section III B we will give a sketch of how this analysis could be extended to a more detailed analysis using wave mechanics.

We assume a setup similar to the one in Fig. 1 which involves cold neutrons traveling at  $v \sim 10^3$  ms<sup>-1</sup> with the mean lifetime  $\tau_n = 880$  s or about 15 minutes. Suppose a ring-like guide with radius  $r$  can be manufactured which makes neutrons follow a circular path  $C$ . According to neutron optics, this can be achieved by using material whose Fermi potential  $V_F$  is such that if neutrons approach the surface of the guide at grazing incidence with small angle  $\theta$ , they are reflected by the potential of the material. Reflection occurs if the kinetic energy  $E$  corresponding to the normal component of the velocity is smaller than the Fermi potential of the material. In other words, for total reflection  $E$  must satisfy the Fermi-Zinn condition  $E \sin^2 \theta < V_F$ . For instance, for a typical material Ni with  $V_F = 250$  neV, the angle  $\theta < 0.3$  deg for neutrons at  $v = 10^3$  ms<sup>-1</sup>. It is important to note that, because the Fermi potential is spin independent, the reflection does not change the spin state [24].

This means that in the neutron optics approach the circular path is approximated by a polygon. The number of vertices of the polygon depends on the angle at which the particle approaches the surface: smaller angle results in higher number

<sup>1</sup> Note that the last equality in (14) is simply obtained by using the explicit form of the holonomy matrix (12) for the case under consideration.

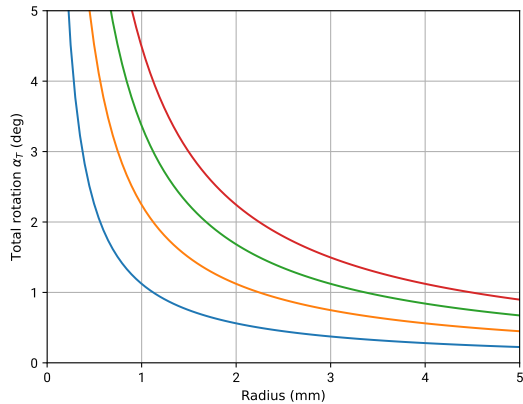


FIG. 2. Dependence of the total Wigner rotation  $\alpha_T$  on the radius  $r$  of circle for a particle with  $v = 10^3 \text{ ms}^{-1}$ , and duration of experiment  $t$  is  $4\tau_n$  (blue),  $8\tau_n$  (yellow),  $12\tau_n$  (green) and  $16\tau_n$  (red).

of vertices and vice versa. As the number of vertices grows, the polygon approaches a circle.

Assuming the circular neutron guide has radius  $r$ , the particle makes  $vt/2\pi r$  revolutions in time  $t$ . Multiplying this with the angle  $\alpha(v)$  per one revolution in (13), we obtain the total rotation

$$\alpha_T = \frac{vt}{2\pi r} \cdot \alpha(v). \quad (15)$$

Plot of  $\alpha_T$  for cold neutrons with  $t = 4\tau_n$  as well as longer times is shown in Fig. 2. This shows different parameter regimes are possible. For instance, a total spin rotation of about 1.1 deg can be observed when the duration of experiment is  $8\tau_n$  and the guiding ring radius is 2 mm. This is close to the precision of 1 deg achievable in a standard configuration.<sup>2</sup> Since the total rotation is proportional to the duration of the experiment, the effect will be twice as large at about 2.2 deg for experiments that last twice as long, and even larger for longer times. Note that at  $8\tau_n$  the duration of the experiment exceeds neutron mean lifetime by eight times, which results in loss of signal. Although this is a restriction it is not a critical issue as long as the resulting signal can be detected.<sup>3</sup>

For an example of how the same total rotation angle of 1.1 deg can be achieved in a different parameter regime, note that the total rotation angle  $\alpha_T$  is proportional to speed  $v$  and experiment time  $t$ , and inversely proportional to radius  $r$  of the guide. Thus increasing speed to  $2 \cdot 10^3 \text{ ms}^{-1}$  while reducing experiment time to  $\tau_n$  also yields the result 1.1 deg. Because now the experiment time is equal to the mean lifetime of neutrons the resulting signal would be significantly

stronger. On the other hand, larger speed means creating suitable beam width and divergence is more challenging because the critical angle must be less than 0.1 deg in this regime.

In summary, we see that while in principle the parameters can be controlled, which allows for different regimes of implementation, the latter also pose different restrictions and challenges for realizing the experiment.

## B. Wave mechanics

In the above description of the experiment, we used two different approaches to describe the two different degrees of freedom of coordinate and spin. We modeled spin evolution in terms of differential geometry; this allowed for an efficient computation of Wigner rotation. On the other hand, we treated spatial propagation using neutron optics. This is justified by the relatively large wavelength of cold neutrons in comparison to interatomic distance. However, a more detailed and accurate approach is to describe spatial propagation in terms of quantum wave mechanics. Such an approach has been taken in [26–28]. In this section, we will briefly describe this work and then comment on the extent to which the same approach can be adopted for our experiment. A more thorough quantitative analysis remains to be carried out in the future.

In the wave mechanics picture, neutrons are described as matter waves that propagate in a potential well formed by the repulsive Fermi potential of the curved guide and the effective centrifugal potential [27]. Whereas [27] assume the neutron guide has the shape of a quarter (or a smaller segment) of a circle, we assume a ring-like waveguide  $C$ . The Schrödinger equation describing the situation remains the same as in [26]. The particle's dynamics is described in cylindrical coordinates  $(\rho, \phi)$  in the plane of the figure, where  $\rho$  is radial distance and  $\phi$  is the angle. The states of the neutrons moving parallel to the surface of the guide have angular momentum which is close to the classical value. The latter justifies approximating the angular coordinate  $\phi$  as a classical continuous variable and describing the propagation along  $\phi$  using classical expression

$$\phi = \frac{vt}{r}. \quad (16)$$

However, the radial dependence displays quantum behavior. The most significant aspect of radial motion for the purposes of our experiment is the existence of deeply bound states in the potential well formed by the effective centrifugal potential and the Fermi potential of the guide. These states are quasistationary since there is a small probability they will tunnel through the potential barrier. The radial dependence of neutron states in the triangular shaped potential well in the vicinity of the curved guide can be found by solving the Schrödinger equation for the potentials in question [26]. Treating  $\phi$  as classical variable, one obtains an expression for the neutron flux describing the evolution of wave packet in the vicinity of the curved guide. The existence of deeply bound quasi-stationary states has been experimentally confirmed in [27].

The importance of this for our experiment is as follows. Whereas in [26, 27] the curved mirror has the shape of a seg-

<sup>2</sup> Better precision has been obtained in an experiment in [25].

<sup>3</sup> Free neutron decay is described by  $N(t) = N(0)e^{-t/\tau_n}$ , where  $N(0)$  is the initial number of neutrons. This means after time period  $t = 2\tau_n$  about 13% of the initial population remains, while only 0.03% is left after  $8\tau_n$  has passed. Whether or not the final population of neutrons can be measured at the end of the experiment depends on the detector sensitivity and the initial size of the neutron population.

ment of circle, in our setup the curved waveguide is a full circle. The formal description in terms of the Schroedinger equation remains the same and so we expect the results of such an analysis to yield states with a structure similar to those described in the above mentioned works. However, we note that the coordinate and spin will be still described by two different formalisms: the spatial propagation in terms of Schroedinger equation and the spin rotation using the differential geometric formalism. The two formalisms complement each other. While the wave mechanics theory can be used to estimate the flux of neutrons that leave the apparatus, the differential geometric approach provides information about the total spin rotation angle.

### C. Challenges

Although neutron experiments have achieved a high level of sophistication, the experiment described above remains challenging because it demands parameter regimes that seem to go beyond the current level of techniques. In this section, we briefly discuss the difficulties that arise along with prospects of mitigating the issues. We hope this will inspire further analysis and technological developments.

The primary concern is the large number of revolutions that neutrons must complete in order to achieve the observable 1 deg of total spin rotation at the end of the experiment. Depending on the implementation parameters, a single revolution produces a minuscule spin rotation of  $\sim 10^{-9} - 10^{-8}$  deg, which requires about  $\sim 10^8 - 10^9$  revolutions to reach 1 deg of spin rotation. In the neutron optics approach this requires that the neutron survive the large number of reflections in the circular waveguide; neutrons that approach the guide at a larger angle than the critical angle  $\theta$  will be absorbed. In the wave mechanics picture this translates into the question of how large is the flux of neutrons leaving the circular waveguide after experiment time  $t$  has passed.

The requirement that only neutrons with grazing incidence under the critical angle  $\theta$  contribute to the experiment severely restricts beam width. Assuming for a moment that the beam is parallel, and the particles enter the curved guide such that the top part of the beam is aligned with the tangent to the perimeter of the curved guide, the critical angle limits the maximum width of the beam to be  $r[1 - \cos(\theta)]$ .<sup>4</sup> For instance, if  $\theta = 0.3$  deg and  $r = 2$  mm, the maximum width is 27 nm. However, in reality the neutron beam has angular divergence; typical divergence  $\Delta\theta$  in neutron experimentation facilities is from 0.5 – 1.0 deg. In this case, the notion of beam width is an approximation since the width increases in the direction of propagation, and it is also useful to consider the angle of acceptance, i.e. the arc that spans the region where particles hit the curved guide. For the parallel beam, the angle of acceptance is  $\theta$ , whereas for the divergent beam it is larger,  $\theta + \Delta\theta$ . The reduction of signal due to the narrow

beam and small critical angle, coupled with long experiment time might make neutron detection extremely challenging. A possible strategy for increasing signal is to increase the critical angle by using neutrons with lower speed. Another is to employ Bragg mirrors, or Ni-Ti super-mirrors which are capable of achieving higher reflection angles.

A further concern is surface roughness. It can be viewed as transforming the velocity component which is parallel to the guiding surface to a component which is normal, thus effectively increasing absorption of neutrons, which ultimately, again, leads to reduction of signal. While a detailed theory of surface roughness can be found in [26] and in references therein, we note that in the realization of the whispering gallery experiment in [28], mirror surface roughness of 0.4 nm was achieved, which was much smaller than the characteristic size of the quantum states involved. We thus assume that surface quality of a guiding ring with such roughness, or even better, can be realized in the experiment.

Lastly, one must take into account external magnetic fields from various sources that lead to systematic errors. For example, the Earth's magnetic field causes Larmor precession of neutron spin. More generally, a wide variety of external sources ranging from nearby machinery to people would all introduce distortions that lead to unwanted effects and errors in sensitive measurements. In order to reduce such effects, the following scheme can be used. First, we assume the experiment is carried out using magnetic shielding techniques. For instance, in [29] the authors report high quality magnetic shielding where residual fields  $B_R$  were observed to be lower than 1 nT. However, a magnetic field of 1 nT would still cause spin precession at several degrees per second, making observation of the significantly smaller Wigner rotation impossible. To counter this, we adopt the following compensation method. We apply a guide field  $B_G$  that defines an axis  $\hat{n}$  of spin rotation. Its magnitude must be large enough so that the angular deviation  $\beta$  from  $\hat{n}$  caused by the residual field is negligible. For this to be true,  $B_R/B_G = \tan\beta$  must be smaller than  $10^{-3}$ . This ensures that even in the worst case when  $B_R$  and  $B_G$  are orthogonal, spin rotation axis is in practice defined by the guiding field. Finally, we use two circular guide rings  $C$ , one where neutrons orbit in the clockwise and the other where they move in the counter-clockwise direction. The axis of the neutrons' circular movement must coincide with the direction of the guide field  $B_G$ . This ensures that, in one direction, the guide-field-induced Larmor precession and Wigner rotation add, whereas in the other direction the Wigner rotation is subtracted from the Larmor rotation. Measuring the final spin rotation of the two streams of neutrons and noting their difference yields the Wigner rotation angle. Incidentally, the scheme halves the required experiment time because the Wigner rotation of 0.5 deg in each direction results in the total difference of 1 deg.

In summary, we believe that by combining the above mentioned strategies progress can be made towards realizing the experiment in the future.

---

<sup>4</sup> We would like to thank an anonymous reviewer for pointing this out.

#### IV. CONCLUSION

We have proposed an experiment that allows to verify Wigner's rotation for massive spin-1/2 particles in the non-relativistic regime with cold neutrons. The reason one can detect Wigner's rotation at these low velocities rests on the cumulative character of the phenomenon: although each revolution around the circle at  $v = 10^3 \text{ ms}^{-1}$  produces a minuscule rotation of  $\sim 10^{-9}$  deg, this can be amplified to an observable 1 deg by letting the particle complete a sufficient number of revolutions. However, the proposed experiment remains challenging at present since it requires parameter regimes that go beyond current level of experimentation techniques. We hope that steady progress in the field will make implementation of the experiment possible in the future.

#### V. ACKNOWLEDGMENTS

We would like to thank the anonymous reviewers for raising a number of important points, as well as for helpful suggestions that improved the quality of the paper. VP acknowledges partial support by the Estonian Research Council (Eesti Teadusagentuur, ETAG) through grants PSG489 and PRG946. CP acknowledges support by the excellence cluster QuantumFrontiers of the German Research Foundation (Deutsche Forschungsgemeinschaft, DFG) under Germany's Excellence Strategy, EXC-2123 QuantumFrontiers, 390837967; support by the German Research Foundation (Deutsche Forschungsgemeinschaft, DFG), Project Number 420243324 and by the Transilvania Fellowships for Visiting Professors grant 2024 of the Transilvania University of Brasov.

---

[1] H. Rauch and S. A. Werner, *Neutron Interferometry* (Clarendon Press, Oxford, 2000).

[2] S. Sponar, J. Klepp, R. Loidl, S. Philipp, K. Durstberger-Rennhofer, R. A. Bertlmann, G. Badurek, H. Rauch, and Y. Hasegawa, *Phys. Rev. A* **81**, 042113 (2010).

[3] Y. Hasegawa, R. Loidl, G. Badurek, M. Baron, and H. Rauch, *Phys. Rev. Lett.* **97**, 230401 (2006).

[4] H. Bartosik, J. Klepp, C. Schmitzter, S. Sponar, A. Cabello, H. Rauch, and Y. Hasegawa, *Phys. Rev. Lett.* **103**, 040403 (2009).

[5] J. Klepp, S. Sponar, and Y. Hasegawa, *Progress of Theoretical and Experimental Physics* **2014**, 082A01 (2014).

[6] S. Sponar, R. I. P. Sedmik, M. Pitschmann, H. Abele, and Y. Hasegawa, *Nature Reviews Physics* **3**, 309–327 (2021).

[7] L. H. Thomas, *Nature* **117**, 514–514 (1926).

[8] R. M. Gingrich and C. Adami, *Physical Review Letters* **89**, 270402 (2002).

[9] A. Peres, P. F. Scudo, and D. R. Terno, *Physical Review Letters* **88**, 230402 (2002).

[10] N. Friis, R. A. Bertlmann, and M. Huber, *Physical Review A* **81**, 042114 (2010).

[11] V. Palge and J. Dunningham, *Annals of Physics* **363**, 275–304 (2015).

[12] A. J. Barr, P. Caban, and J. Rembieliński, *Quantum* **7**, 1070 (2023), arXiv:2204.11063 [quant-ph].

[13] V. Palge and C. Pfeifer, *Physical Review A* **109**, 032206 (2024), arXiv:2310.08121 [quant-ph].

[14] F. R. Halpern, *Special Relativity and Quantum Mechanics* (Prentice-Hall, 1968).

[15] J. P. Costella, B. H. J. McKellar, and A. A. Rawlinson, *American Journal of Physics* **69**, 10.1119/1.1371010 (2001).

[16] J. A. Rhodes and M. D. Semon, *American Journal of Physics* **72**, 943–960 (2004).

[17] F. Wilczek and A. Shapere, *Geometric Phases in Physics*, Advanced Series in Mathematical Physics: Volume 5 (World Scientific, 1989).

[18] H. Lyre, *Studies in History and Philosophy of Science Part B: Studies in History and Philosophy of Modern Physics* **48**, 45–51 (2014).

[19] B. Simon, *Physical Review Letters* **51**, 2167 (1983).

[20] C. Cisowski, J. Götte, and S. Franke-Arnold, *Reviews of Modern Physics* **94**, 031001 (2022).

[21] Y. Hasegawa and G. Badurek, *Physical Review A* **59**, 4614–4622 (1999).

[22] S. Sponar, J. Klepp, C. Zeiner, G. Badurek, and Y. Hasegawa, *Physics Letters A* **374**, 431–434 (2010).

[23] B. Demirel, S. Sponar, and Y. Hasegawa, *New Journal of Physics* **17**, 023065 (2015).

[24] A. T. Boothroyd, *Principles of neutron scattering from condensed matter* (Oxford University Press, 2020).

[25] Y. Hasegawa, C. Schmitzter, H. Bartosik, J. Klepp, S. Sponar, K. Durstberger-Rennhofer, and G. Badurek, *New Journal of Physics* **14**, 023039 (2012).

[26] V. V. Nesvizhevsky, A. K. Petukhov, K. V. Protasov, and A. Y. Voronin, *Physical Review A* **78**, 033616 (2008).

[27] V. V. Nesvizhevsky, A. Y. Voronin, R. Cubitt, and K. V. Protasov, *Nature Physics* **6**, 114–117 (2010).

[28] V. V. Nesvizhevsky, R. Cubitt, K. V. Protasov, and A. Y. Voronin, *New Journal of Physics* **12**, 113050 (2010).

[29] I. Altarev, M. Bales, D. Beck, T. Chupp, K. Fierlinger, P. Fierlinger, F. Kuchler, T. Lins, M. Marino, B. Niessen, *et al.*, *Journal of Applied Physics* **117** (2015).